

CERN LIBRARIES, GENEVA



CM-P00057507

## ASTROPARTICLE PHYSICS

John Ellis

*Theoretical Physics Division, CERN  
CH - 1211 Geneva 23*

A selection of topics in astroparticle physics is reviewed, including inflationary cosmology, evidence for non-baryonic dark matter, a massive neutrino as a candidate for Hot Dark Matter, and the lightest supersymmetric particle as a candidate for Cold Dark Matter. Various possible strategies for detecting supersymmetric relics from the Big Bang are also reviewed.

## 1 Particle Cosmology

### 1.1 Big Bang Cosmology

There are three major pieces of evidence for the Big Bang<sup>?</sup>. One is the present-day *Hubble expansion*: all distant objects in the Universe are receding from one another at velocities  $v$  that increase approximately linearly with the distance  $d$ :

$$v = H \cdot d \quad (1)$$

where  $H$  is the Hubble constant, conventionally expressed as  $H = h \cdot 100$  Km/s/Mpc, where  $h \simeq 0.5$  to 1. Clearly, the larger the value of  $H(h)$ , the younger the Universe, and there has been some concern recently<sup>?</sup> whether determinations of  $h$  are compatible with the present age  $t_0$  of the Universe, as inferred from observations of globular clusters:  $t_0 = 14 \pm 3$  Gy, and even white dwarfs in our galaxy:  $t_0 > 9 \pm 2$  Gy. My own view is that there is no significant conflict: recent determinations of  $H$  indicate<sup>?</sup> that

$$H = 66 \pm 13 \text{ km/s / Mpc} \quad (2)$$

where I have allowed for a (somewhat arbitrary) error of 20 %. This seems relatively conservative, in view of all the steps involved in going from (for example) a simple observation of Cepheid variables in Leo I to a value of  $h$ . As you can see in Fig. 1, there is no *a priori* conflict between the range (2) and the apparent age of the Universe.

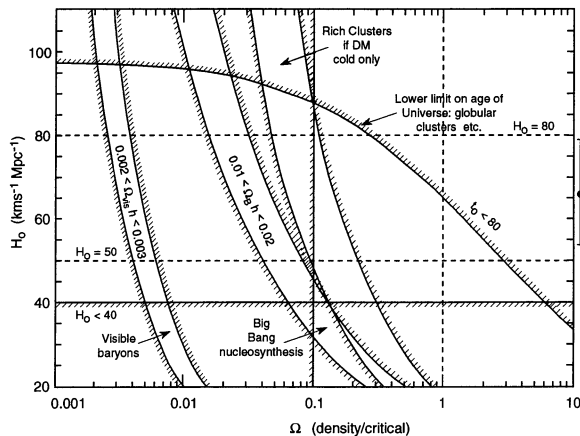


Figure 1: The  $(\Omega, H_0)$  plane, adapted from <sup>7</sup>, which exhibits no serious discrepancy between the average measured value of  $H_0$ ,  $\Omega = 1$ , and an age for the Universe of  $10^{10}$  years. This plot also shows the estimates of the present baryon density  $\Omega_{baryons}$  obtained from visible features in the Universe, from Big Bang Nucleosynthesis and from rich clusters. All the indications are that  $\Omega_{baryons} \lesssim 0.1$ , so that at least 90% of the matter in the Universe is non-baryonic dark matter.

The second major piece of evidence for Big Bang cosmology is provided by the *Microwave Background Radiation*. This is thought to be a relic of the (re)combination of nuclei and electrons to form atoms, which would have occurred when the temperature of the Universe was about 1000 times larger than the effective temperature  $T_0 \simeq 2.73$  K of the background radiation today, and the scale size  $a$  of the Universe was  $\simeq 1000$  times smaller. The high degree of uniformity of this radiation is the best evidence we have for the essential isotropy of the Universe: we will come later to the fluctuations in the microwave background radiation that were observed recently by COBE and other experiments.

The third major piece of evidence for the Big bang is provided by the *Light Element Abundances*<sup>7</sup>, which are highly consistent with nuclear cooking when the Universe was about  $10^9$  times hotter than it is today, corresponding to particle energies between 0.1 and 1 MeV. They are consistent with observation if the number of light neutrino species is 3 or 4, and the relative abundance of baryons

$$\frac{n_B}{n_\gamma} \sim 10^{-10} \text{ to } 10^{-9} \quad (3)$$

which would correspond to a density of baryons far below the critical density  $\rho_c$ , beyond which the Universe would be fated to cease its present expansion and collapse in a Big Crunch.

Most of the theories of cosmological inflation discussed in the next section predict that the overall density of the Universe should be very close to this critical value. Therefore, if the estimate (3) were correct, it would imply that most of the matter in the Universe must be non-baryonic dark matter. Hence it is important to review critically the strength of the arguments leading to the estimate (3), to see whether there is any loophole in it.

There has recently been considerable controversy<sup>7</sup> concerning the abundance of Deuterium, which is a very fragile nucleus, and hence particularly sensitive to reprocessing within stars, leading to an interest in measurements at high redshift, which should be closer to the primordial cosmological abundance. Different high-redshift measurements currently yield discrepant deuterium abundances, and hence favour different ranges of  $n_B$ . However, even the lower estimates of the Deuterium abundance are not compatible with  $\rho_B \simeq \rho_c$ . Moreover, high values of the baryon density are disfavoured by measurements of  ${}^4\text{He}$  and  ${}^7\text{Li}$ <sup>7</sup>.

The success of Big Bang Nucleosynthesis takes us back to when the Universe was  $\simeq 10^8$  times smaller and hotter than it is today. Before going back further in time, let us review briefly the formalism of homogeneous and isotropic Friedman-Robertson-Walker cosmology. The Hubble expansion rate is governed by

$$H^2 \equiv \left(\frac{\dot{a}}{a}\right)^2 = \frac{8\pi G_N}{3} \rho - \frac{k}{a^2} \quad (4)$$

where  $k = 0$  or  $\pm 1$  is the curvature of the Universe,  $G_N \equiv 1/M_P^2$ :  $M_P \simeq 1.2 \times 10^{19}$  GeV is Newton's constant, and  $\rho$  is the total density of matter in the Universe. If  $k = 0$ , the Universe is flat and the density is critical:  $\rho = \rho_c$ ,

$$H = \sqrt{\frac{8\pi G_N}{3} \rho_c} \quad (5)$$

and  $\rho_c \simeq 2 \times 10^{-29} h^2 \text{ g/cm}^3$  numerically.

It is believed that the density of the Universe today is dominated by non-relativistic particles, but that at early epochs it was usually dominated by relativistic particles in thermal equilibrium<sup>7</sup>:

$$\rho = \frac{\pi^2}{30} T^4 g \quad : \quad g = \#_B + \frac{7}{8} \#_F \quad (6)$$

leading to a Hubble expansion rate  $H \simeq T^2/M_P$ . In the Standard Model,

$$\#_B = 4 + (8 \times 2) + (4 \times 2) \quad (7)$$

where the three terms represent the gluons, weak vector bosons and Higgs bosons, respectively, and

$$\#_F = 30 \times N_g \quad (8)$$

where the number of generations  $N_g = 3$ , presumably.

The above formulae apply if thermal equilibrium has been established, but was this in fact the case in the early Universe? To answer this question, we need to compare the Hubble expansion rate with typical interaction rates, such as

$$\Gamma \sim \alpha T, \quad \frac{\alpha^2}{T^2} \cdot T^3 \quad (9)$$

for  $1 \rightarrow 2$ ,  $2 \rightarrow 2$  processes, respectively. Equilibrium is established if  $H < \Gamma$ , which is likely to have been the case for  $T \ll M_P$ ?. This is an important result, which implies, for example, that phase transitions in the early Universe can be treated using quasi-equilibrium methods, except possibly for the onset of inflation. Since baryogenesis requires a breakdown of thermal equilibrium?, it could only have occurred during one of these phase transitions, and even then only if it was first order.

We conclude this section by discussing the last of these phase transitions to have occurred, namely the transition from the initial quark-gluon plasma to the present hadronic phase of strongly-interacting matter. If this transition was first order, there could have been substantial supercooling or remnants of the quark-gluon phase, leading to inhomogeneities in the early Universe, centred on nucleation sites for the new hadronic vacuum. It has been suggested? that these might have provided a loophole in the picture of homogeneous nucleosynthesis presented above, leading perhaps to a relaxation of the crucial upper bound on  $n_B$ , and possibly even allowing the baryon density to reach the critical density and obviate the need for non-baryonic dark matter.

This scenario could have been effective only if the distance between hadronic nucleation sites was larger than the length  $\delta R$  over which protons could have diffused at that epoch, which was about 0.5 m. Most estimates of the QCD phase transition parameters indicate that it was at most weakly first order? ?, so that such a large value of  $\Delta R$  seems rather unlikely. Moreover, as seen in Fig. 2, inhomogeneous nucleosynthesis calculations are strongly constrained by the observed light element abundances, making it difficult to deviate far

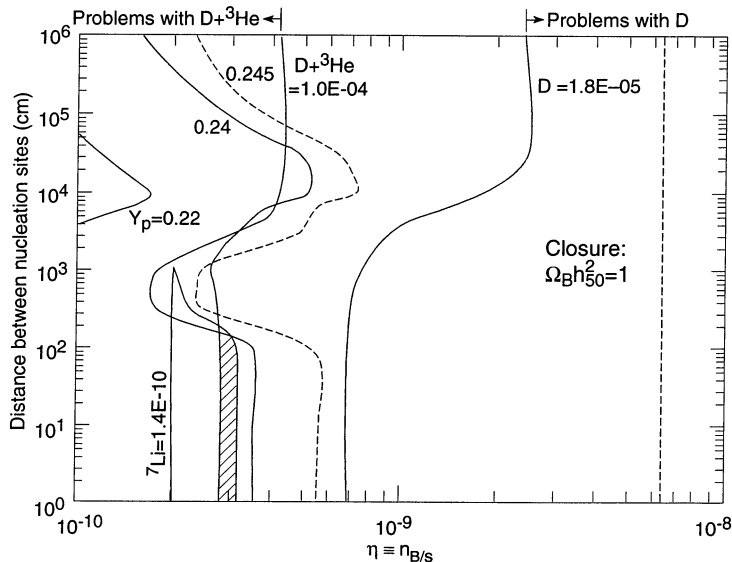


Figure 2: Constraints on inhomogeneous Big Bang nucleosynthesis models imposed by the observed light element abundances<sup>?</sup>.

from the homogeneous analysis presented above<sup>?</sup>. Accordingly, the previous estimate of  $n_B$  seems rather robust, and the need for non-baryonic dark matter established, if one accepts the standard inflationary scenario presented in the next section.

## 1.2 Introduction to Inflation

The motivations for inflation<sup>?</sup> are provided by a number of puzzles thrown up by the standard Big Bang theory. One is the *Horizon/Smoothness Problem*. Opposite parts of the Universe which are only just now becoming visible, i.e., coming within our apparent horizon, look very similar, in the sense that cosmic Microwave Background Radiation from their different directions has almost identical temperatures:

$$\left(\frac{\delta T}{T}\right)_{CMBR} \simeq 10^{-5} \quad (10)$$

to which should be added the apparently increasing uniformity of the distribution of matter (galaxies) over larger distance scales. These similarities hold

despite the fact that, in conventional Big Bang cosmology, these distant regions could never have been in causal contact earlier in the history of the Universe, since no light wave or other message could have travelled between them. This is because the scale size  $a$  of the Universe grows as

$$a \propto t^{1/2} \text{ or } t^{2/3} \quad (11)$$

for a Universe whose energy density is dominated by relativistic or non-relativistic matter, respectively. The expansion rate (11) is much smaller than the naive horizon size  $a_H \propto t$ . If no message could have been transmitted between them, how did these distant regions of the Universe know how to behave with such military coordination (10)?

Secondly, there is the *Flatness/Oldness Problem*. We can write (4) in the form

$$H^2 = \left(\frac{\dot{a}}{a}\right)^2 = \frac{8\pi}{3}G_N\rho - \frac{k}{a^2} \quad (12)$$

and define  $\Omega \equiv \rho/\rho_c$ , where  $\rho_c$  is given by (5). Equation (12) then tells us that

$$\Omega(t) = \frac{1}{\left(1 - \frac{3k}{8\pi G_N \rho a^2}\right)} \quad (13)$$

where  $\rho \propto a^{-4}(a^{-3})$  for a radiation-(matter-)dominated Universe. The geometries of cosmological models with different values of  $k$  are as follows:  $k < 1$  is an open Universe that expands for ever,  $L > 1$  a closed Universe that eventually collapses in a Big Crunch, and  $k = 1$  is the critical case where the space-time geometry is flat, as in traditional Euclidean geometry.

We see from (13) that if  $\Omega \simeq 1$  today, as seems observationally to be the case, then  $\Omega$  must have been exceedingly close to unity early in the history of the Universe. Specifically, one may estimate that

$$\Omega - 1 \lesssim 10^{-60} \quad \text{when } t = 10^{-43} \text{ s} \quad (14)$$

if conventional Big Bang cosmology applied unmodified all the way back to that epoch. This apparent fine tuning makes it a puzzle why  $\Omega$  is quite close to unity nowadays. Another way of phrasing this puzzle is: how come the Universe has succeeded in keeping  $\Omega$  in the ballpark of unity until such a ripe old age? A generic solution of the expansion equation (4) would have  $t_P = M_P^{-1}$  as its characteristic time scale. How has our Universe escaped this fate?

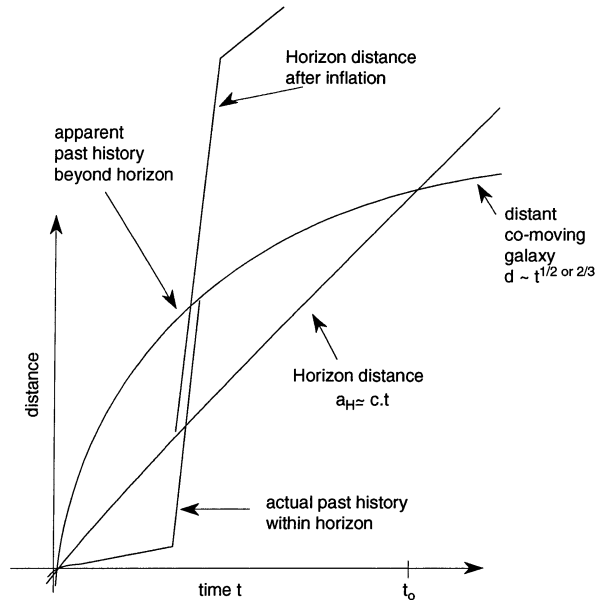


Figure 3: The horizon and the history of a distant galaxy at rest in a comoving reference frame, in conventional Big Bang cosmology and in inflationary cosmology.

The basic idea of inflation<sup>7</sup> is that at some early epoch the expansion rate of the Universe may have been dominated by a (more or less) constant term:  $\rho = V$ . It is easy to check that in this case the Universe would have expanded exponentially:

$$a \simeq a_0 e^{Ht} : H = \sqrt{\frac{8\pi}{3} G_N V} \quad (15)$$

Such an epoch of rapid expansion would have caused the *horizon* to expand exponentially, as seen in Fig. 3. If this went on for sufficiently long time:  $\Delta t \gtrsim 60/H$ , the entire observable Universe would have been within the pre-inflationary horizon, making possible the establishment of homogeneity in the very early Universe. Inflation would mean that the true horizon is exponentially large, much larger than the naive horizon  $a_H = t$ , as also seen in Fig. 3.

This epoch of exponential expansion would also have solved the *flatness* problem, because the curvature terms  $-k/a^2$  would have become negligible. This exponential approach towards a flat Universe explains why  $\Omega$  is now so close to unity, despite the old age of the Universe: most inflationary models

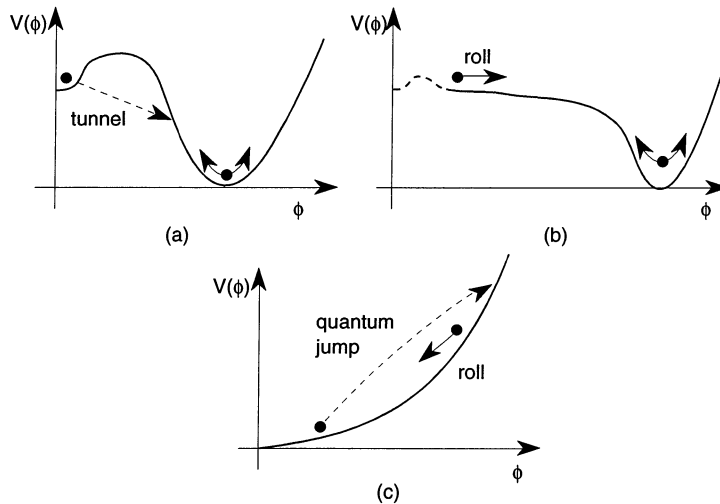


Figure 4: The behaviour of the Higgs field in (a) old inflation<sup>?</sup>, (b) new inflation<sup>?</sup>, and (c) a chaotic inflationary model<sup>?</sup>.

predict that  $\Omega - 1 \lesssim 10^{-4}$ . This explains why Euclidean geometry is such a good approximation in our Universe!

### 1.3 Inflationary Models

The *Old Inflation* model<sup>?</sup> postulated that the exponential expansion was driven by the field energy tied up in some inflaton scalar field  $\phi$  that was stuck in a false vacuum, namely a local minimum of the potential  $V(\phi)$  with non-zero vacuum energy, as seen in Fig. 4a. Eventually, quantum effects cause the  $\phi$  field to tunnel through the bump in the potential  $V$  and down to the global minimum with zero vacuum energy. During inflation, there is an effective cosmological constant

$$\Lambda = 8\pi G_N V(\phi = 0) \quad (16)$$

and the Hubble expansion rate

$$H = \sqrt{\frac{8\pi G_N}{3} V} \quad (17)$$



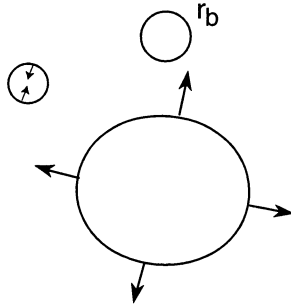


Figure 5: In a first-order transition, bubbles of the new vacuum are surrounded by a “cheese” made of the false vacuum. Bubbles smaller than the critical size  $r_b$  contract, whilst larger bubbles expand.

The trouble with this model was that the phase transition to the true vacuum would never have been completed<sup>?</sup>: as illustrated in Fig. 5, the bubble-like regions of the new vacuum would be surrounded by domains of the old vacuum that were still expanding exponentially. If there were sufficiently many bubbles to have a chance of filling the Universe, the tunneling rate to the true vacuum would have to be so rapid that there would not be enough expansion in the inflationary phase:  $H/\Delta t \ll 60$ .

One possible fix was provided by *New Inflation*<sup>?</sup>, which postulated a  $V$  that was sufficiently flat that enough inflation would occur after the transition out of the false vacuum, as illustrated in Fig. 4b. According to this scenario, we live in a bubble of the true vacuum, that is larger than the entire visible Universe, but probably surrounded by regions of false vacuum that are still expanding exponentially. A feature of this model is that  $H$  is not quite constant during inflation, which implies that the inflationary perturbations to be discussed shortly are not quite scale invariant.

It is not in fact necessary to postulate the existence of such a false vacuum: according to models of *Chaotic Inflation*<sup>?</sup>, a generic monotonically-decreasing potential such as

$$V(\phi) \simeq \phi^n \quad \text{or} \quad e^{\alpha\phi} \tag{18}$$

would provide adequate inflation if it were flat enough. In this type of model, there would always be parts of the Universe where quantum fluctuations would drive the value of the  $\phi$  field sufficiently far up the potential for enough inflation to take place during the subsequent roll down the hill, as seen in Fig. 4c.

#### 1.4 Perturbations in the Early Universe

The basic mechanism for generating inhomogeneities in inflationary cosmology is that of quantum fluctuations in the scalar field  $\phi$ : since  $\phi$  has different initial values in different places, it rolls down the potential at different speeds, and different parts of the Universe expand at different rates<sup>?</sup>. Assuming that these perturbations are small, they lead to a Gaussian random field of fluctuations  $\delta\rho/\rho$  and hence temperature variations  $\delta T/T$  which is almost independent of the scale size, as wanted by astrophysicists. The magnitude is generally proportional to the field energy during the inflationary expansion:

$$\frac{\delta\rho}{\rho} \propto \mu^2 G_N \quad (19)$$

This is consistent with the observations of COBE and other experiments if  $\mu \simeq 10^{16}$  GeV: is it mere coincidence that this is close to the calculated scale of supersymmetric grand unification?

There are in general two types of inflationary perturbations<sup>?,?</sup>: density or scalar perturbations, and gravity or tensor perturbations. In the former case, one considers the density field  $\rho(\mathbf{x})$  and its fluctuations

$$\delta(\mathbf{x}) = \frac{\rho(\mathbf{x}) - \langle \rho \rangle}{\langle \rho \rangle} \quad (20)$$

with Fourier transform  $\delta_k$ , related to density perturbations on a scale  $\lambda$  by

$$\left(\frac{\delta\rho}{\rho}\right)_\lambda^2 = \frac{k^3 \delta_k^2}{2\pi^2} \quad (21)$$

where  $\lambda = k^{-1}$ . The evolution of these perturbations depends on the ratio  $\lambda/a_H$ . If  $\lambda/a_H < 1$ , the evolution depends on astrophysical dynamics, such as the nature of matter, its equation of state, dissipation, etc:

$$\ddot{\delta}_{\mathbf{k}} + 2H\dot{\delta}_{\mathbf{k}} + v_s^2 \frac{k^2}{a^2} \delta_{\mathbf{k}} = 4\pi G_N \langle \rho \rangle \delta_{\mathbf{k}} \quad (22)$$

where  $v_s^2 = dp/d\rho$  is the speed of sound. If the wave number  $k > k_J$ :

$$k_J^2 = \frac{4\pi G_N a^2 \langle \rho \rangle}{v_s^2} \quad (23)$$

the fluctuation grows. Specifically, in the case of Cold Dark Matter, for which  $v_s \simeq 0$ , perturbations grow on all scales as soon as they come within the horizon

$a_H$ . On the other hand, if  $\lambda/a_H > 1$ , the gauge-invariant ratio  $\delta\rho/(\rho + p)$  is time-independent. Hence its value generated by inflation is the same as the value when this perturbation comes back within the horizon  $a_H$ .

During inflation,

$$\delta\rho = \delta\phi \times V'(\phi), \quad \rho + p \simeq \langle \dot{\phi}^2 \rangle \quad (24)$$

whilst the rollover of the inflaton field is controlled by the equation

$$\dot{\phi} + 3H\dot{\phi} + V'(\phi) = 0 \quad (25)$$

If the rollover is slow, so that  $\dot{\phi}$  is negligible,

$$\dot{\phi} \simeq -\frac{V'(\phi)}{3H} \quad (26)$$

whereas the conventional quantum fluctuations of the scalar field in de Sitter space imply

$$\delta\phi \simeq \frac{H}{2\pi} \quad (27)$$

Combining these results, we find that

$$\frac{\delta\rho}{\rho} + p \simeq \frac{\delta\phi V'(\phi)}{\dot{\phi}^2} \simeq \frac{H^3 V'}{(V')^2} \simeq \frac{V^{3/2}}{V'} \quad (28)$$

Since this quantity remains unchanged until the perturbation returns within the horizon, we conclude that

$$\left(\frac{\delta\rho}{\rho}\right)_{\lambda=a_H} \equiv A_S(\phi) = \frac{\sqrt{2}\kappa^2 H^2}{8\pi^{3/2} H'} : \kappa^2 \equiv 8\pi G_N \quad (29)$$

On the other hand, the gravity-wave (tensor) perturbations are controlled by the massless wave equation in curved space:

$$\ddot{h}_k^{1,2} + 3H\dot{h}_k^{1,2} + \frac{k^2}{a^2} h_k^{1,2} = 0 \quad (30)$$

for the two graviton polarization states  $h_k^{1,2}$ , where we have decomposed the metric into a Friedman-Robertson-Walker background and a perturbation:  $g_{\mu\nu} = g_{\mu\nu}^{FRW} + h_{\mu\nu}$ , and Fourier-analyzed the latter. The magnitude of these tensor perturbations is also unchanged outside the horizon, and have the initial values?

$$h_k^{1,2} \simeq \frac{H}{2\pi} \quad (31)$$

We therefore have

$$A_G(\phi) \equiv (k^3 h_k) \lambda = a_H = \frac{\kappa}{4\pi^{3/2}} H \quad (32)$$

Comparing (??) and (??), we see that

$$\frac{A_S(\phi)}{A_G(\phi)} = \frac{\kappa}{\sqrt{2}} \frac{H}{H'} \quad (33)$$

It is easy to see that this ratio exceeds unity if  $\dot{a} > 0$ , which is clearly the case if the inflaton is accelerating down the potential hill. However, the relative contributions of gravity waves and scalar perturbations to large-angle anisotropies in the cosmic microwave background radiation are given approximately by  $25A_G^2/2A_S^2$ ?, so gravity waves may still be important for the interpretation of the COBE signal.

The relations (??) and (??) may also be used to reconstruct the inflationary potential from observations of perturbations?. The height of the potential is given by

$$\frac{V}{M_P^4} = \frac{75}{32} A_G^2 \left[ 1 + 0.21 \frac{A_G^2}{A_S^2} \right] \quad (34)$$

whilst its slope is given by

$$\frac{V'}{M_P^3} = -\frac{75\sqrt{\pi}}{8} \frac{A_G^3}{A_S} [1 - 0.85A_G^2 - 0.53n_S] \quad (35)$$

and its curvature, which is essentially the squared mass of the inflaton, is

$$\frac{V''}{m_p^2} = \frac{25\pi}{4} A_G^2 \left[ n_s + 6 \frac{A_G^2}{A_S^2} - 16 \frac{A_G^4}{A_S^4} - \frac{n_S^2}{6} - 9.8n_s \frac{A_G^2}{A_S^2} + 1.1 \frac{dn_s}{d \ln k} \right] \quad (36)$$

where  $n_{S,G}$  are the spectral indices of the scalar and gravity waves, which would be unity for scale-invariant spectra.

Measurements of fluctuations in the microwave background were first made by the COBE satellite?, and 4-year sky maps are now available?. The COBE determinations of multipoles of the fluctuation spectrum are consistent with a scale-invariant spectrum?:

$$n = 1.1 \pm 0.3 \quad (37)$$

Also, the COBE measurements are consistent with the observed fluctuations being Gaussian?, as predicted by inflation. this has been tested by studies of

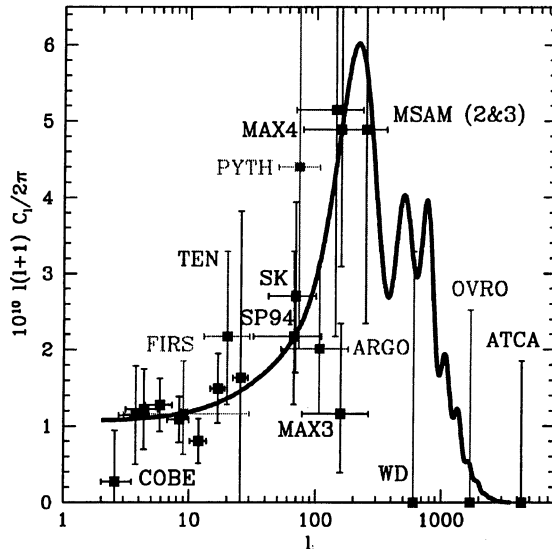


Figure 6: Compilation of data on fluctuations in the cosmic microwave background spectrum<sup>?</sup>, which provides the basis for a discussion of theoretical ideas and observational issues in measuring fluctuations in the cosmic microwave background radiation. The harmonic number  $l \propto 1/d$ .

the 3-point correlation function, by looking at the topologies of hot and cold regions, and by comparisons with constrained models.

The COBE measurements have been confirmed and complemented by many other experiments<sup>?</sup>, as seen in Fig. 6. Also shown for comparison is a spectrum calculated in a Cold Dark Matter model with  $h = 0.5$  and  $\Omega_b = 0.05$ . this model predicts a first Döppler peak at  $l \simeq 200$ , followed by secondary peaks and finally a drop off at large  $l$  due to the thickness of the last scattering surface. the height of the first peak would increase with  $\Omega_b$ , and it would shift to higher  $l$  if the total density  $\Omega < 1$ . A combined fit to the data yields<sup>?</sup>

$$n = 1.1 \pm 0.1 \quad (38)$$

and provides an indication of a first Döppler peak near the expected value of  $l$  and with the expected magnitude, though this needs to be confirmed. The fluctuation spectrum will be the object of many detailed studies in the coming years. In particular, two new satellite projects have recently been approved, MAP and COBRAS/SAMBA, which should provide full-sky coverage

with angular resolutions better than  $1/2$  degree and 13 arc minutes, respectively. These should provide exhaustive tests of inflationary models and precise measurements of cosmological parameters.

## 2 RUNNING HOT AND COLD DARK MATTER

### 2.1 How Much Dark Matter?

Averaged over the Universe as a whole, naturalness and the inflationary cosmology discussed in the previous lecture suggest that  $\Omega = 1$ . On the other hand, astrophysical observations find  $\Omega_{visible} \simeq 0.003$ , and the Big Bang nucleosynthesis arguments reviewed in the previous lecture suggest that  $\Omega_B \lesssim 0.1$ . Observations of galactic rotation curves suggest that their halos contain  $\Omega_{Halo} \simeq 0.1$ . Thus, mathematically all the halos could be composed of baryons.

The most prominent candidates for a baryonic component in the halo of our galaxy are “brown dwarfs”, objects with masses below  $\sim 0.08$  of the solar mass. Initial observations by the EROS and MACHO collaborations<sup>?</sup> indicated that most of our galactic halo was not composed of such objects. However, the MACHO collaboration has recently released<sup>?</sup> the data from their second year, which contain more microlensing events and have greater sensitivity to longer time scales, i.e., heavier masses. Taken together, these indicate a greater optical depth of brown dwarfs, corresponding to a larger fraction of our halo  $f \sim 1/2$ , although this is difficult to reconcile with the EROS observations. Moreover, the MACHO observations require a rather bizarre mass function for halo objects<sup>?</sup>. The objects they see would have masses around  $1/2$  of the solar mass, suggesting that they are “white dwarfs”. However, the progenitors of white dwarfs would have had masses above about twice the solar mass. No objects in this range, or in the range between  $0.1$  and the solar mass (“red dwarfs”) have been seen.

The local halo density has recently been re-estimated<sup>?</sup> allowing for the possibility of a somewhat flattened halo:

$$\rho_{DM} \simeq 0.51_{-0.17}^{+0.21} \text{ GeV cm}^{-3} \quad (39)$$

If this estimate is correct, there must be a significant local density of Cold Dark Matter, even if our halo is infested with brown dwarfs, and we will use for subsequent purposes the estimate  $\rho_{DM} \simeq 0.3 \text{ GeV cm}^{-3}$ . In any case, Cold Dark Matter is required for structure formation, as we now review.

## 2.2 Hot or Cold Dark Matter?

These terms refer to particles that are relativistic or non-relativistic when structures such as galaxies and clusters began to form in the early Universe. Which you prefer depends on your favourite theory of galaxy formation. If you pursue the Gaussian random field of density perturbations suggested by inflation, then you should prefer the predominance of Cold Dark Matter, since this enhances the growth of perturbations on all scales up to the horizon size. On the other hand, Hot Dark Matter escapes from small-scale perturbations, implying that galaxies form (too) late<sup>?</sup>. For this reason, inflationary perturbations with Cold Dark Matter has been regarded as a “Standard Model” of structure formation, and will be pursued in the rest of this lecture. You should be aware, however, that an alternative possibility is that structures in the Universe originated from small-scale seeds such as cosmic strings<sup>?</sup>, for which Hot Dark Matter is to be preferred, since Cold Dark Matter would have led to too much power on small scales.

Recent data<sup>?</sup> indicate that the paradigm of inflationary perturbations with Cold Dark Matter may require some modification: this is particularly apparent when one compares data on large-scale perturbations from COBE with data from smaller scales (IRAS, APM, etc.). One possibility is an admixture of Hot Dark Matter, resulting in the cocktail<sup>?</sup>

$$\Omega_{Cold} \simeq 0.7, \quad \Omega_{Hot} \simeq 0.2, \quad \Omega_B \lesssim 0.1 \quad (40)$$

In this scenario, the most natural candidate for the hot component of the dark matter would be a massive neutrino with  $m_\nu \sim 10$  eV. Another possibility is that there is a non-zero cosmological constant  $\Lambda$ , but I see no natural origin for this from the point of view of particle theory, and will not discuss it further. A third possibility is to postulate pure Cold Dark Matter but with a perturbation spectrum which is tilted. However, this latter model tends to predict fluctuations that are too large on intermediate scales.

Figure 7 shows the relic density for a generic “neutrino” or other massive neutral particle. When the mass  $\leq 1$  MeV, the number density is almost independent of the mass and hence  $\rho_\nu \propto m_\nu$ . The resulting  $\Omega_\nu$  exceeds unity when  $m_\nu \simeq 30$  eV. The cosmological density falls back below unity again when  $m_\nu \gtrsim 3$  GeV<sup>?</sup>, as annihilation through the Z boson becomes more efficient. The relic density may rise again towards unity if  $m_\nu \lesssim M_Z/2$ , if the annihilation rate is given by a canonical point-like cross-section.

In this case, there is an approximate upper limit on the possible mass of a

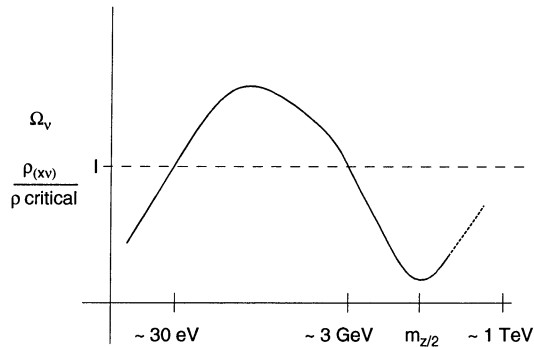


Figure 7: Qualitative picture of the neutrino relic density  $\rho_\nu$  as a function of the neutrino mass  $m_\nu$ .

Cold Dark Matter particle in the context of conventional Big Bang cosmology<sup>?</sup>. The present mass density

$$\Omega_X = \frac{\rho_X}{\rho_{crit.}} \simeq \frac{m_X n_X}{2 \times 10^4 h^2 T_0^2} \quad (41)$$

where  $T_0 \simeq 2.73K$  is the present-day black-body temperature. The comoving number density of particles would have been approximately constant since annihilation ended (freeze out):

$$\frac{n_X}{T_0^3} \simeq \frac{n(T_f)}{T_f^3} : n(T_f) < \sigma v > \simeq \frac{\dot{R}_f}{R_f} \simeq \frac{T_f^2}{M_P} \quad (42)$$

where  $m_X/T_f \simeq 20-30$  in many models. This implies that

$$\Omega_X h^2 \simeq \frac{1}{10^3 < \sigma v >} \frac{1}{2.7K \times M_P} \simeq \frac{1}{10^3 < \sigma v >} \times \frac{1}{1\text{TeV}^2} \quad (43)$$

Note the remarkable coincidence in the second part of the denominator in this equation! Using  $< \sigma v > \sim \mathcal{O}(\alpha^2/m_X^2)$ , one may estimate

$$m_X \sim 16\alpha \sqrt{\frac{\Omega_X h}{0.25}} \text{ TeV} \leq 1 \text{ TeV} \quad (44)$$

which is almost a “guaranteed” discovery for the LHC. Looking at fig. 7, we see three general collisions where  $\Omega_\nu \sim 1$ , namely  $m_\nu \sim 30$  eV, in which case the relic would constitute Hot Dark Matter, and  $m_\nu \sim 3$  GeV or 1000 GeV, in which cases it would constitute Cold Dark Matter. Neutrinos would inhabit the first of these ecological niches, supersymmetric particles one of the others.



### 2.3 Massive Neutrinos

Particle experiments<sup>?</sup> indicate that neutrinos are much lighter than quarks and leptons:

$$m_{\nu_e} \leq 4.5 \text{ eV}, \quad m_{\nu_\mu} \leq 160 \text{ KeV}, \quad m_{\nu_\tau} \leq 23 \text{ MeV}. \quad (45)$$

Theoretically, there is no reason to expect neutrino masses to vanish, and they are indeed expected in Grand Unified Theories. The simplest possibility, which we shall explore in the following, is a generic see-saw mass matrix<sup>?</sup>:

$$(\nu_L, \nu_R) \begin{pmatrix} m_{\nu_L} & m_q \\ m_q & m_{\nu_R} \end{pmatrix} \begin{pmatrix} \nu_L \\ \nu_R \end{pmatrix} \quad (46)$$

whose diagonalization leads naturally to very light neutrinos

$$m_{\nu_e} \sim \frac{m_q^2}{M_{\nu_R}} \leq m_{q,\ell} \quad (47)$$

These non-zero masses would be accompanied by non-zero flavour mixing angles à la Cabibbo-Kobayashi-Maskawa. The off-diagonal entries in (??) would be conventional Dirac mass terms, analogous to those for conventional quarks and leptons and originating from the Higgs boson of the Standard Model. The diagonal entries would be Majorana masses, which are only possible for neutrinos. There could in principle be such a mass term for the left-handed neutrino  $\nu_L$ , but this would require violation of lepton number:  $\Delta L = 2$  and weak isospin  $\Delta I = 1$ . There is no corresponding Higgs field in the Standard Model or in the minimal SU(5) GUT, but it can appear in more complicated models. Such a Majorana term could also appear via a non-renormalizable coupling of the form<sup>?</sup>:

$$\frac{1}{M} \left( H_{\Delta I=\frac{1}{2}} \nu_L \right) \left( H_{\Delta I=\frac{1}{2}} \nu_L \right) \quad (48)$$

where  $M$  is a large mass parameter, which could originate from the exchange of a heavy right-handed neutrino  $\nu_R$ . The bottom-right and diagonal entry in Eq. (??) represents a Majorana mass for  $\nu_R$ , which is expected to be of order  $M_{GUT}$  in many models. The appearance of off-diagonal Dirac masses in Eq. (??) suggests a natural hierarchy

$$m_{\nu_e} : m_{\nu_\mu} : m_{\nu_\tau} \simeq m_u^2 : m_c^2 : m_t^2 \quad (49)$$

with flavour mixings related to the Cabibbo-Kobayashi-Maskawa matrix.

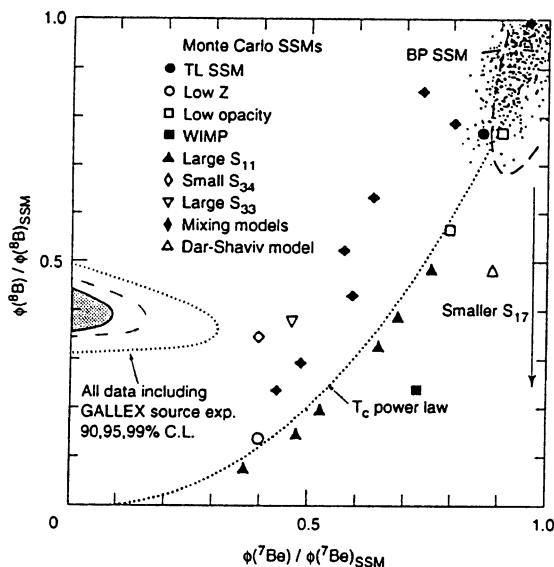


Figure 8: A planar presentation<sup>?</sup> of the solar neutrino deficits seen in different experiments, compared with a selection of different solar models.

There are several experimental indications for non-zero neutrino masses, of which the most serious is the **Solar Neutrino Deficit**. By now, this has been seen in five experiments (Homestake, Kamioka, SAGE, GALLEX<sup>?</sup> and Superkamioka<sup>?</sup>), and cannot be explained away simply by reducing the central temperature of the Sun. This would not explain the observational fact that Boron neutrinos are suppressed less than Beryllium neutrinos, as seen in Fig. 8<sup>?</sup>, and would also conflict with helioseismological observations. There are several plausible interpretations in terms of neutrino oscillations, namely the matter-enhanced (Mikheyev-Smirnov-Wolfenstein<sup>?</sup>) scenario

$$\Delta m^2 \sim 10^{-5} \text{ eV}^2, \quad \sin^2 2\theta \sim 10^{-2} \quad (50)$$

the large-angle solution

$$\Delta m^2 \sim 10^{-5} \text{ eV}^2, \quad \sin^2 2\theta \sim 1 \quad (51)$$

and the vacuum solution

$$\Delta m^2 \sim 10^{-10} \text{ eV}^2, \quad \sin^2 2\theta \sim 1 \quad (52)$$

My favourite among these scenarios is (??), in particular since the mixing angles required in the other scenarios are surprisingly large. If we take (??) seriously, then in agreement with (??), presumably

$$m_{\mu e} \leq m_{\mu\nu} \sim 2 \text{ or } 3 \times 10^{-3} \text{ eV} \quad (53)$$

The see-saw mechanism (??) then suggests that

$$m_{\nu\tau} \sim \frac{m_t^2}{m_c^2} m_{\nu\mu} \sim 1 \rightarrow 10 \text{ eV} \quad (54)$$

making the  $\nu_\tau$  an ideal candidate for the Hot Dark Matter required in the mixed Dark Matter scenario (??) ?.

The **Atmospheric Neutrino Deficit** ? seen by the Kamioka and IMB experiments requires further confirmation, in my view, in particular by experiments using a different technique. The anomaly seen by the **LSND** experiment also requires a confirmation from other experiments.

The hypothesis that the  $\nu_\tau$  be the Hot Dark Matter in the Universe may be subject to tests by on-going accelerator experiments ?; if the  $\nu_\mu \rightarrow \nu_\tau$  mixing angle is in a range  $10^{-4} - 10^{-2}$ . This is quite a generic possibility in the context of the solar neutrino parameters (??) and the see-saw mechanism (??).

A value of  $m_{\nu\tau}$  in the range (??) requires a right-handed neutrino mass  $M_{\nu_R}$  around  $10^{12}$  GeV, which happens to gibe nicely with a promising GUT scenario for baryogenesis ?. This is often thought to be due to the out-of-equilibrium decays of massive GUT particles such as gauge bosons  $X$  or Higgs bosons  $H_X$  with  $\Delta B \neq 0$  couplings:  $X(H_X) \rightarrow qq, \bar{q}\ell$ . If these decays exhibit C- and CP-violating asymmetries:  $b = p(X \rightarrow qq) \neq \bar{b} = p(\bar{X} \rightarrow \bar{q}\bar{q})$ , they can produce a net quark asymmetry

$$\frac{n(q) - n(\bar{q})}{n(q) + n(\bar{q})} = \frac{3(b - \bar{b})}{2 + b + \bar{b}} \quad (55)$$

which would have persisted until the quark/hadron phase transition, at which time the  $\bar{q}$  would have annihilated, leaving a surplus of  $q$  to provide the baryons we know and love.

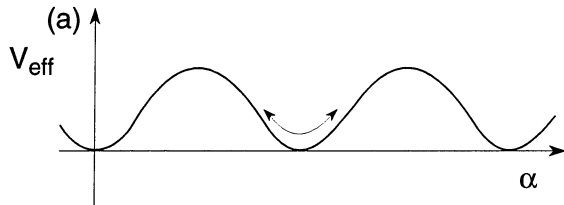


Figure 9: The effective potential for the Chern-Simons vacuum parameter  $\alpha$ .

This scenario has required modifications after the realization that non-perturbative electronic interactions violate baryon number. These arise from the fact that the electroweak gauge theory vacuum is complicated, being labelled in particular by the Chern-Simons number  $\alpha$  as shown in Fig. 9. The barriers between the different vacua are described by unstable sphaleron solutions<sup>?</sup> of the electroweak field equations with masses

$$M_{sph} \simeq \frac{M_W(T)}{\alpha} \simeq 10 \text{ TeV} \quad (56)$$

Transitions across these barriers occur with rates of order

$$e^{-\beta M_{sph}} \quad (57)$$

where the sphaleron mass is given by (??). This rate is expected to be large at temperatures above the electroweak phase transition. Furthermore, the sphaleron transition is accompanied by correlated changes in the baryon and lepton numbers:

$$\Delta B = N_G = 3 = \Delta L \quad (58)$$

Note that the combination  $B - L$  is conserved, whereas we expect

$$(B+L) \simeq -c(B+L)T \quad (59)$$

This has no suppression factor and is expected to be in equilibrium at high  $T$ , tending to drive  $B + L \rightarrow 0$ .

Any GUT scenario for baryogenesis should therefore generate a primordial  $B - L$  asymmetry. One attractive scenario for this is the decay of a heavy  $\nu_R$ , which may produce a lepton asymmetry:  $\nu_R \rightarrow \nu_L + H$ <sup>??</sup>. Any such  $L$  asymmetry would be recycled by non-perturbative electroweak effects to yield a non-zero baryon asymmetry  $B \neq 0$ . For this scenario to work, the  $\nu_R$  must

be produced after inflation, and the most promising possibility is in inflaton decay. This requires that the  $\nu_R$  be lighter than the inflaton, which is suggested by the density perturbations  $\delta\rho/\rho$  seen by COBE to be  $\leq 10^{13}$  GeV. Inserting this value into (??) suggests that  $m_{\nu\tau} \gtrsim 1$  eV, in encouraging convergence with the indications from the matter-enhanced interpretation (??) of the solar neutrino deficit and the mixed dark matter scenario (??).

Those of you who are interested in the detection of Cold Dark Matter will be interested in the local density of  $\nu_\tau$  in our galactic halo<sup>?</sup>. The usual scenario for galaxy formation involves the quasi-spherical infall of dark matter particles, which occupy a hypersheet in phase space that wraps around itself in layers. The phase-space density of fermions is limited by  $1/2 (2\pi)^3$ , and the neutrino velocity is limited by the velocity of escape from our galaxy, so that

$$\rho_{\mu_{halo}} \leq \rho_{\mu_{max}} = \frac{1}{2(2\pi)^3} g_\nu \frac{4\pi}{3} (10^{-3} c)^3 m_\nu^4 \quad (60)$$

This provides quite a stringent upper limit on the function of a galactic halo that may be in the form of neutrinos: for typical numbers  $m_\nu = 9$  eV,  $h = 0.55$  corresponding to  $\Omega_\nu = 0.3$ , we estimate  $\Omega_{\nu_{halo}} < 0.048$ <sup>?</sup>. We conclude that most of our galactic halo does not consist of Hot Dark Matter particles, and we earlier concluded that most of it could not be baryonic, so let us now consider one of the most plausible candidates for its Cold Dark Matter component.

#### 2.4 Lightest Supersymmetric Particle?

This is expected to be stable in many supersymmetric models, and hence present in the Universe today as a cosmological relic from the Big Bang, thanks to a multiplicatively-conserved quantum number called  $R$  parity, which takes the values<sup>?</sup> +1 for all particles and -1 for all sparticles. The conservation of  $R$  parity is related to those of baryon and lepton numbers and spin  $S$ :

$$R = (-1)^{3B+L+2S} \quad (61)$$

Needless to say,  $R$  violation is possible if, for example,  $L$  is violated either spontaneously or explicitly, but the type of  $L$ -violating neutrino masses discussed in the previous section does not violate  $R$  parity. If it is indeed conserved, it has three important consequences

- Sparticles are always produced in pairs, such as  $pp \rightarrow \tilde{q}\tilde{q}X$  or  $e^+e^- \rightarrow \tilde{\mu}^+\tilde{\mu}^-$ ,

- Heavier sparticles decay into lighter ones, for example  $\tilde{q} \rightarrow q\tilde{g}$ ,  $\tilde{\mu} \rightarrow \mu\tilde{\gamma}$ , and the
- Lightest sparticle is absolutely stable, because it has no legal decay mode.

If this supersymmetric relic had electric charge or strong interactions, it would have condensed into galaxies, stars and planets where it would have bound to nuclei and now be detectable as an anomalous heavy isotope. None of these have ever been seen at levels far below the abundance calculated for supersymmetric relics. We therefore conclude that any supersymmetric relic is probably electromagnetically neutral and can have only weak interactions. The available scandidates in the sparticle data bookino include the sneutrino  $\tilde{\nu}$  of spin 0, the neutralino  $\tilde{\chi}$  which is a combination of the  $\tilde{\gamma}/\tilde{H}/\tilde{Z}$  at spin 1/2, and the gravitino  $\tilde{G}$  of spin 3/2. The first of these has not been seen at LEP or by experiments searching directly for dark matter scattering on nuclei, and is presumably excluded, whilst the gravitino seems essentially undetectable and will therefore be ignored in the next lecture.

### 3 NEUTRALINO DETECTION STRATEGIES

#### 3.1 Cosmological Neutralino Density

The properties of neutrinos and charginos are characterized by three parameters at the tree level, namely the unmixed gaugino mass  $m_{1/2}$ , the Higgs superpotential mixing parameter  $\mu$  and the ratio of Higgs vacuum expectation values  $\tan\beta = v_2/v_1$ . The neutralino mass matrix is<sup>?,?</sup>:

$$\begin{pmatrix} M_2 & 0 & \frac{-g_2 v_2}{\sqrt{2}} & \frac{g_2 v_1}{\sqrt{2}} \\ 0 & M_1 & \frac{g' v_2}{\sqrt{2}} & \frac{-g' v_1}{\sqrt{2}} \\ \frac{-g_2 v_2}{\sqrt{2}} & \frac{g' v_2}{\sqrt{2}} & 0 & \mu \\ \frac{g_2 v_1}{\sqrt{2}} & \frac{-g' v_1}{\sqrt{2}} & \mu & 0 \end{pmatrix} \quad (62)$$

where it is conventional to assume that the SU(2) and U(1) gaugino masses are related by universality at the GUT scale

$$M_2 = M_1 = m_{1/2} \quad (63)$$

which are renormalized at lower scales:

$$M_2 : M_1 = \alpha_2 : \alpha_1 \quad (64)$$

The neutralino mass matrix (??) simplifies in the limit  $m_{1/2} \rightarrow 0$ , in which the lightest supersymmetric particle  $\chi \simeq \tilde{\gamma}$ , and in the limit  $\mu \rightarrow 0$ , in which  $\chi \simeq \tilde{H}$ . However, experimental constraints from LEP and elsewhere tell us<sup>?</sup> that

$$m_\chi \gtrsim 20 \text{ GeV} \quad (65)$$

as we discuss later in more detail. One of the most appealing features of the neutralino dark matter candidate is that there are generic domains of parameter space where an “interesting” cosmological density in the range  $\Omega h^2 \simeq 0.1$  to 1 is possible<sup>?</sup>, even including this experimental constraint.

The experimental constraints from LEP in the  $\mu, M_2$  plane are shown in Fig. 10 for the representative case  $\tan \beta = \sqrt{2}$ . We notice a certain complementarity between the limits from running at the  $Z^0$  peak (LEP 1) and from higher-energy running (LEP 1.5). These are reflected in Fig. 11, where we see that LEP 1 data alone do not establish a rigorous lower limit on the  $m_\chi$ , nor do data from LEP 1.5 alone, but their combination does<sup>?</sup>. The limit  $m_\chi \gtrsim 13$  GeV given in<sup>?</sup> is purely experimental, but relies on the assumption that  $m_{\tilde{\nu}} = 200$  GeV, and even in this case there is a loop-hole for  $\tan \beta < 1.02$ . There is an even larger loop-hole for smaller values of  $m_{\tilde{\nu}} \sim 60$  GeV when  $\tan \beta \sim \sqrt{2}$ . These loop-holes can be plugged by implementing other experimental constraints, and strengthened by requiring that the relic density of neutralinos be in the cosmologically interesting range and/or imposing the theoretical constraint of dynamical electroweak symmetry breaking<sup>?</sup>, as seen in Fig. 12.

The density of a massive relic particle such as the neutralino is controlled by the annihilation rate in the early Universe<sup>??</sup>

$$\frac{dn}{dt} = - 3 \frac{\dot{a}}{a} n - \langle \sigma_{ann} v \rangle (n^2 - n_0^2) \quad (66)$$

where for many cases of interest,

$$\langle \sigma_{ann} v \rangle \simeq a + bx : x \equiv \frac{\langle v^2 \rangle}{6} \quad (67)$$

where  $v$  is the  $\chi$  velocity at annihilation. There is an approximate solution to (??) for  $n(t)$  which is obtained by assuming that  $n = n_0$  (the equilibrium

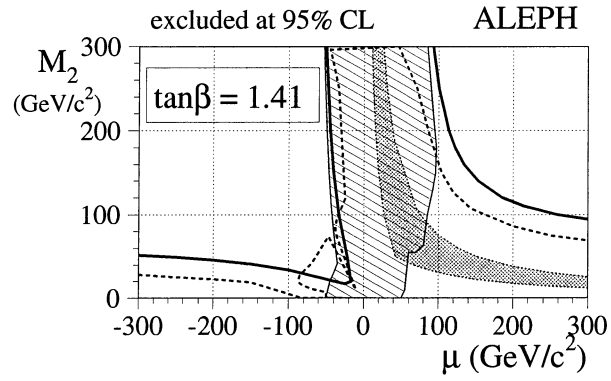


Figure 10: The region of the  $(\mu, M_2)$  plane excluded by<sup>7</sup> on the basis of searches for charginos and neutralinos at LEP1 and LEP 1.5.

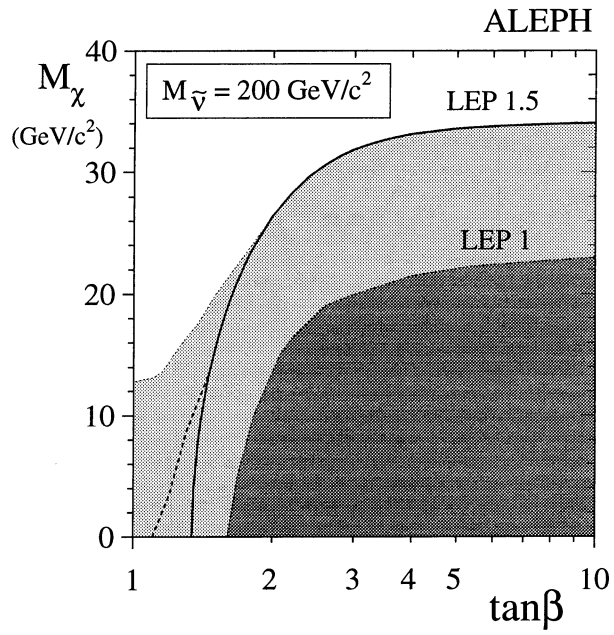


Figure 11: Experimental lower bound<sup>7</sup> on the neutralino mass: note that neither LEP 1 nor LEP 1.5 data by themselves impose a non-zero lower bound.



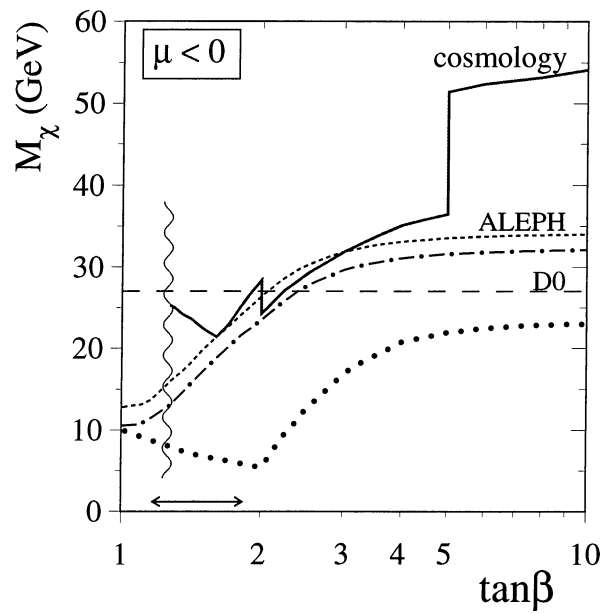


Figure 12: The lower bound in the previous figure (which actually vanishes in the region indicated by the double arrow) is compared with results obtained<sup>?</sup> by imposing additional experimental constraints (dotted line) and cosmological considerations (dash-dotted and solid lines: the latter includes an assumption of dynamical electroweak symmetry breaking). Also shown<sup>?</sup> is a horizontal dashed line obtained from a search for gluinos by the D0 collaboration, and a vertical wavy line beyond which dynamical electroweak symmetry breaking is no longer possible.

density) until  $\dot{n}_0 \sim \langle \sigma_{ann} v \rangle n_0^2$  at the freeze-out temperature  $T_f$ , after which  $\dot{n} \sim \langle \sigma_{ann} v \rangle n^2$ . This freeze-out approximation leads to a present mass density

$$\rho \simeq 0.8 (T_\chi)^3 \frac{m_\chi}{ax_f + \frac{1}{2}bx_f^2} \quad (68)$$

where the prefactor of 0.8 corrects the approximation and the effective  $\chi$  temperature,  $T_\chi$  is given by

$$\left(\frac{T_\chi}{T_\gamma}\right)^3 \sim \left(\frac{g_{eff}(T_f)}{g_{eff}(lowE)}\right)^{-\frac{3}{4}} \quad (69)$$

where  $g_{eff}(T_f)$  is the number of effective relativistic degrees of freedom at the freeze-out temperature, and  $T_\gamma \sim 2.73$  K. In useful units, Eq. (??) yields

$$\rho \sim 4.0 \times 10^{-40} \left(\frac{T_\chi}{2.8^0 K}\right)^3 N_{eff}^{\frac{1}{2}} \left(\frac{\text{GeV}^{-2}}{ax_F + \frac{1}{2}bx_f^2}\right) g \text{ cm}^{-3} \quad (70)$$

The annihilation coefficients  $a, b$  are computable in the model<sup>?,?</sup>, being determined by exchanges of heavy particles such as the  $Z^0$ , sparticles and Higgs bosons. The latter are characterized by two parameters, which may be taken to be a Higgs mass and  $\tan \beta$ , at the tree level, but also depend on  $m_t$  at the one-loop level.

Figure 13 displays the supersymmetric relic density calculated in a sampling of phenomenological models in which universal gaugino and squark/slepton/Higgs masses are assumed at the GUT scale<sup>?</sup>. Among the deviant neutralino possibilities studied recently is the case where scalar masses are not universal<sup>?</sup>: for example, the Higgs masses might differ from the other scalar sparticle masses:

$$m_{H_i}^2 = m_0^2 (1 + \delta_i) \quad (71)$$

In this case, the preferred neutralino composition may change from being mainly a gaugino to mainly a Higgsino, as seen in Fig. 14a, and the annihilation and interaction rates differ from the standard universal scenario. Another deviant possibility<sup>?</sup> is that of large CP violation in the neutralino sector, which would lead to enhanced S-wave annihilation and permit larger neutralino masses as seen in Fig. 14b.

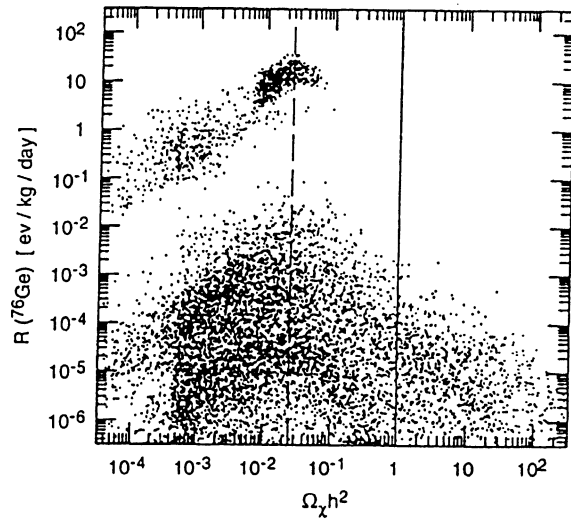


Figure 13: Relic density of supersymmetric particles, calculated in a sampling of different models<sup>?</sup>, together with the estimated scattering rate on  $^{76}\text{Ge}$ .

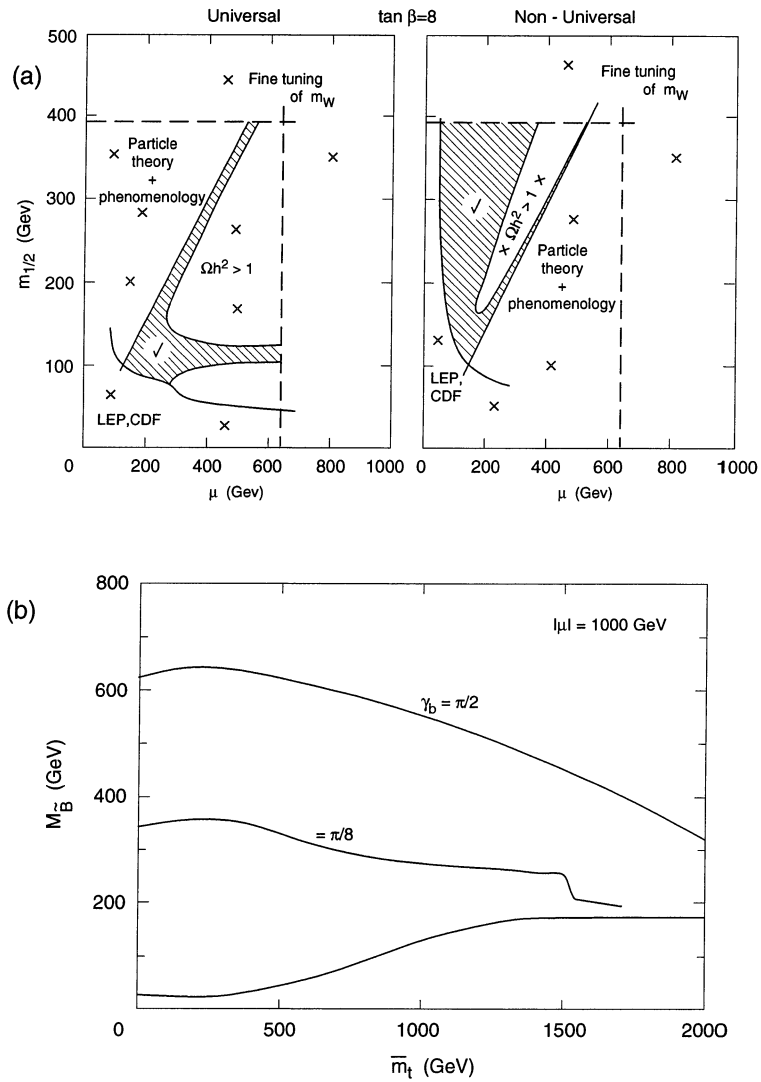


Figure 14: Some results of relaxing the usual restrictive assumptions made in analyses of supersymmetric relic particles: (a) the supersymmetric relic is more likely to be a higgsino if scalar masses are not universal<sup>?</sup>, and (b) it may be heavier if there are large CP-violating phases<sup>?</sup>.

### 3.2 Annihilation in the Galactic Halo

If our galactic halo is indeed largely composed of neutralino, every once in a while a pair of them will find each other and have a one-night stand annihilation<sup>?</sup>, producing  $\bar{l}l, \bar{q}q$ , etc., and thereby detectable stable particles such as the  $\bar{p}, e^+, \gamma$  and  $\nu$  in the cosmic rays. A compilation of recent data on the measured  $\bar{p}$  flux, compared with new calculations of the flux of  $\bar{p}$  to be expected as secondary products of primary matter cosmic rays, and with (optimistic) supersymmetric model calculations, indicates that the data agree perfectly with the conventional production mechanism, and we infer that it will be difficult to observe neutralino dark matter in this way. The same is true of recent measurements of the cosmic-ray positron fraction compared with calculations of conventional production mechanisms. Once again, recent measurements do not confirm previous reports that disagreed with these standard calculations. I also am not optimistic that a neutralino signal could be extracted from future  $e^+$  measurements. Finally, let me mention the possibility that exclusive  $\chi\chi \rightarrow \gamma + \dots$  annihilation processes might yield a detectable monochromatic  $\gamma$  signal in some specific models<sup>?</sup>.

### 3.3 Annihilation in the Sun or Earth

During its wanderings around the galaxy, a neutralino  $\chi$  may pass through the Sun or Earth, collide with a resident nucleus and lose sufficient recoil energy for its orbit to be converted from hyperbolic to elliptic. Since its perihelion (perigee) would be below the radius of the Sun (Earth), it would return many more times, suffering repeated scattering and energy loss, and eventually settling into a quasi-isothermal distribution in the core of the Sun (Earth). The local population would be controlled by annihilation<sup>??</sup>, since the evaporation rate is negligible for  $m_\chi > \text{few GeV}$ , as required by LEP experimental data. Such annihilations in the Sun are expected to be in equilibrium with the trapping rate, but this may not be true in the case of the Earth. Annihilations would yield high-energy neutrinos  $\chi\chi \rightarrow \nu + \dots$ , which might be detectable either directly in an underground experiment or indirectly via the production of muons in the surrounding rock. The high-energy  $\nu$  event rate from the Sun is given by

$$R_\nu \simeq 2.7 \times 10^{-2} \times f \left( \frac{m_{\tilde{\gamma}}}{m_p} \right) \times \left( \frac{\sigma(\tilde{\gamma}p \rightarrow \tilde{\gamma}p)}{10^{-40} \text{ cm}^2} \right)$$

$$\begin{aligned}
& \times \left( \frac{\rho_{\tilde{\gamma}}}{0.3 \text{ GeV cm}^{-3}} \right) \times \left( \frac{300 \text{ km s}^{-1}}{\bar{v}} \right) \\
& \times \sum_i a_i \sum_f B_f \langle N_Z \rangle_{fi} \left( \frac{\text{events}}{\text{kt.year}} \right) \tag{72}
\end{aligned}$$

where the first algebraic factor is kinematical, the next is the elastic  $\chi p \rightarrow \chi p$  scattering cross-section, the next two factors include the local halo density and mean neutralino velocity respectively, and the last factor depends on neutrino physics known from accelerator experiments.

The elastic scattering cross-sections  $\sigma(\chi p/n \rightarrow \chi p/n)$  are mediated by the same heavy particles as control the cosmological annihilation rate (??). The dominant contribution relevant to high-energy solar neutrinos is the spin-dependent amplitude  $A$ , which in the case  $Q \simeq \tilde{\gamma}$  takes the form<sup>?</sup>

$$A = \sum_q e_q^2 \Delta q \tag{73}$$

where the  $\Delta q$  are the contributions to the proton spin of the different quark flavours. These have now been measured relatively precisely in polarized lepton-nucleon scattering experiments:

$$\begin{aligned}
\Delta u &= 0.82 \pm 0.03 \pm \dots \\
\Delta d &= -0.44 \pm 0.03 \pm \dots \\
\Delta s &= -0.11 \pm 0.03 \pm \dots
\end{aligned} \tag{74}$$

and disagree significantly with the predictions of naïve quark models.

Figure 15 shows a scatter plot of the possible rates of muon production by neutralino annihilation in the Sun in a sampling of phenomenological models<sup>?</sup>. We see that a detector with an area of  $1 \text{ km}^2$  has a fair probability of observing these<sup>?</sup>, and even a smaller detector has some chance. However, one word of caution is in order: these high-energy solar neutrinos are also valuable to matter-enhanced oscillation effects, which might convert  $\nu_\mu$  into  $\nu_e$ , which would not produce this clean secondary  $\mu$  signal.

### 3.4 Direct Detection in the Laboratory

This approach is based on the search for the elastic scattering of neutralinos on nuclei<sup>?</sup>: having a typical velocity  $v \simeq 300 \text{ km/s}$ , they would deposit a recoil

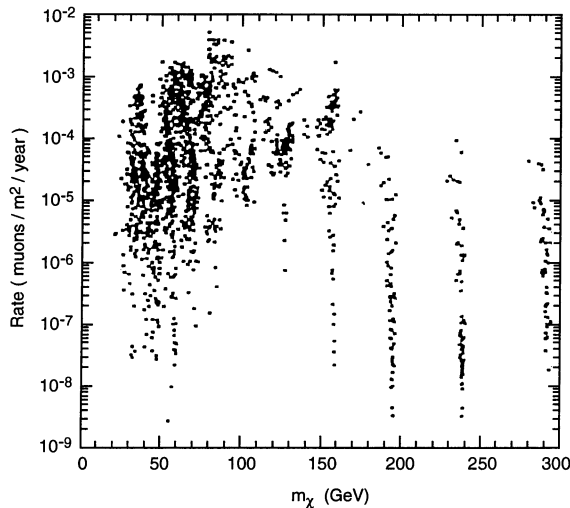


Figure 15: The flux of upward-going muons expected from  $\chi\chi$  annihilation inside the Sun in a sampling of supersymmetric models<sup>?</sup>.

energy

$$\Delta E < \frac{1}{2}m_\chi v^2 \simeq 10 \left( \frac{m_\chi}{10 \text{ GeV}} \right) \text{ keV} \quad (75)$$

The type of spin-dependent interaction discussed above in connection with capture by the Sun would be dominant for nuclear targets with low  $A$ . It would be mediated essentially by  $Z^0$  and  $\tilde{q}$  exchange, and depend on the quark spins in the nucleon (??) and in turn on the contribution of individual nucleon spins to the nucleus, for which the shell model provides a calculational starting point. One also expects a spin-independent interaction mediated by  $H$  and  $\tilde{q}$  exchange, which should be dominant for high- $A$  nuclei, and would depend on the different quark contributions to the nucleon mass. The elastic scattering rate is given in general by

$$R = (R_{SD} + R_{SI}) \left( \frac{4m_\chi m_N}{(m_\chi + m_N)^2} \right) \left( \frac{\rho_\chi}{0.3 \text{ GeV cm}^{-3}} \right) \left( \frac{\langle |v| \rangle}{320 \text{ km s}^{-1}} \right) \quad (76)$$

where formulae for the spin-dependent part  $R_{SD}$  and the spin-independent part  $R_{SI}$  can be found in<sup>?</sup>.

Simple shell-model calculations<sup>?</sup> are expected to be most accurate for nuclei in which there is either a single nucleon outside a closed shell, or there is

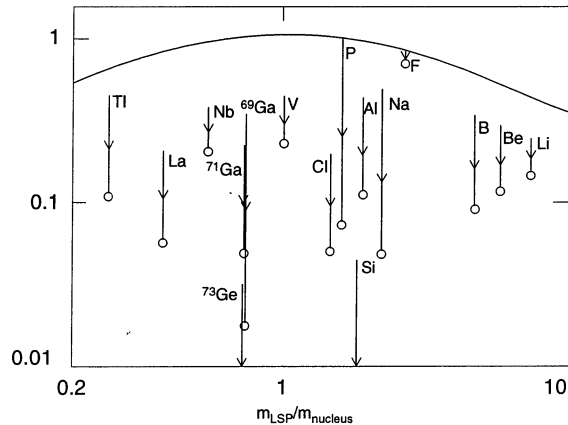


Figure 16: Figures of merit for spin-dependent neutralino-nucleus scattering. The tops of the arrows are the naïve shell-model predictions, the bottoms are those found<sup>?</sup> in the odd-group model<sup>?</sup>.

just one particle hole inside a closed shell. Shell-model predictions are shown in Fig. 16 for a representative collection of possible nuclear targets. It is possible to check the likely accuracy of shell-model calculations by looking at nuclear magnetic moments<sup>?</sup>. It turns out that simple single-particle shell-model calculations are indeed accurate for odd-even or even-odd nuclei close to closed shells, but may be very inaccurate in other cases. Figure 16 also shows the likely reductions in the shell-model estimates obtained using the odd-group model<sup>?</sup>, according to which the nuclear spin is not carried only by the odd nucleon, but is shared among all nucleons of the same species. There are other techniques for improving simple shell-model calculations which have been used in the literature. For example, calculations have been made in a complete basis of shell-model states<sup>?</sup>, but these are restricted for practical reasons to relatively light nuclei. There are also pairs of mirror nuclei which can be used to decompose the amounts of nuclear spin carried by both the odd and even species<sup>?</sup>. All these techniques agree that  $^{19}\text{F}$  should be favoured among light nuclei, as seen in Fig. 16, and that its nuclear matrix elements may be estimated quite reliably.

In addition to these factors, one must also worry about nuclear form factors<sup>?</sup>, which are increasingly important for heavier neutralinos. In the case of the spin-independent interaction, the mass form factor may be estimated using



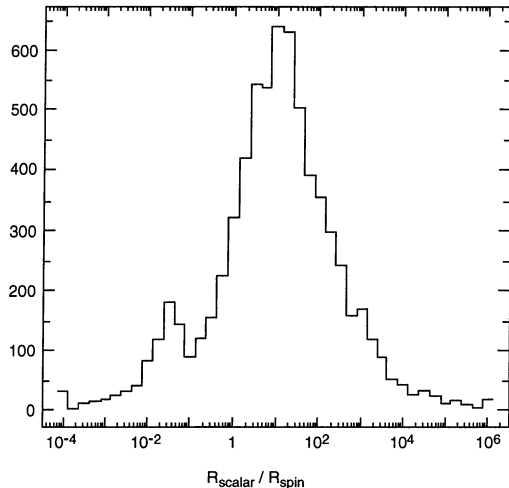


Figure 17: A comparison of the spin-dependent and spin-independent interaction rates of relic neutralinos  $\chi$  with Germanium in a sampling of supersymmetric models <sup>?</sup>.

a Fermi model, according to which there is a non-Gaussian skin around the nucleus. However, the appropriate spin-dependent form factor is more open to debate: one expects that there will be at least one node in the form factor, but its location is uncertain. Figure 17 compares the spin-independent and spin-dependent scattering rates for  $^{73}\text{Ge}$  in a sampling of supersymmetric models, obtained taking all the above effects into account <sup>?</sup>. We see that the spin-independent mechanism is likely to dominate, but this is not certain.

Figure 18 shows typical scattering rates for various nuclei, assuming that the cosmological neutrino density is in the interesting range:  $0.1 < \Omega_\chi h^2 < 1$ , for two different assumed values of the pseudoscalar Higgs mass  $m_A$ . One expects in general an anticorrelation between the cosmological relic density and the Ge scattering rate, as seen in Fig. 13: models with large scattering rates tend to have low cosmological relic densities.

Existing experiments to search for dark matter are already biting into the parameter space of supersymmetric models. Figure 19 compares the present sensitivities of direct and indirect searches for neutralino dark matter with the rates expected in models (a) with and (b) without universality assumed. We have every reason to hope that new experiments looking for neutralino dark matter – either directly via its elastic scattering on nuclei, or indirectly via

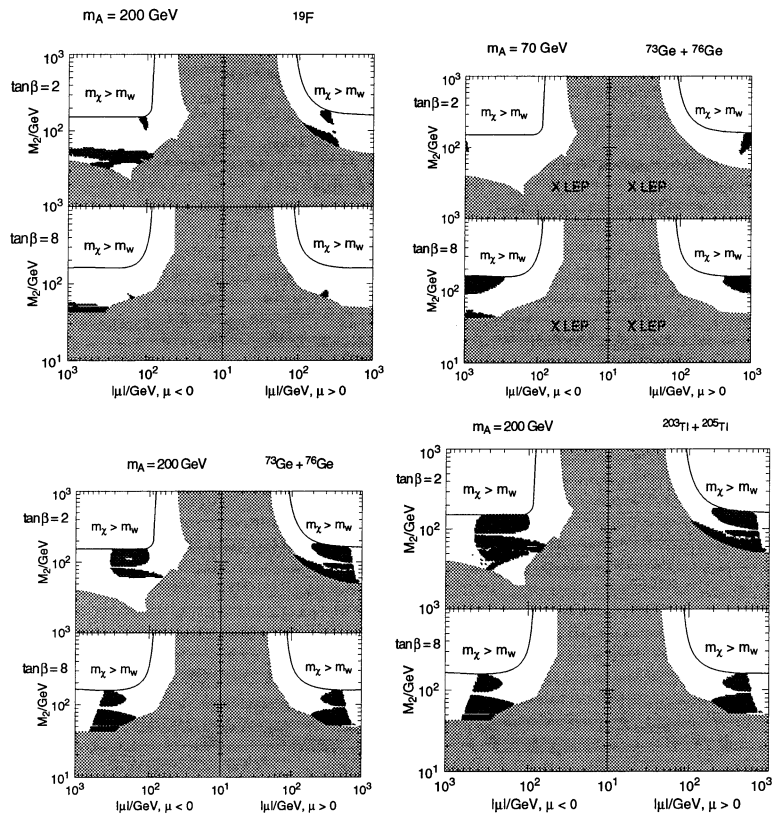


Figure 18: Elastic scattering rates for  $^{19}\text{F}$ ,  $^{73}\text{Ge} + ^{76}\text{Ge}$  and  $\text{Tl}$  for pseudoscalar Higgs masses  $m_A = 70 \text{ GeV}$  and  $200 \text{ GeV}$ . The rates are above  $0.1 \text{ events kg}^{-1} \text{d}^{-1}$  in the shaded regions  $?$ .

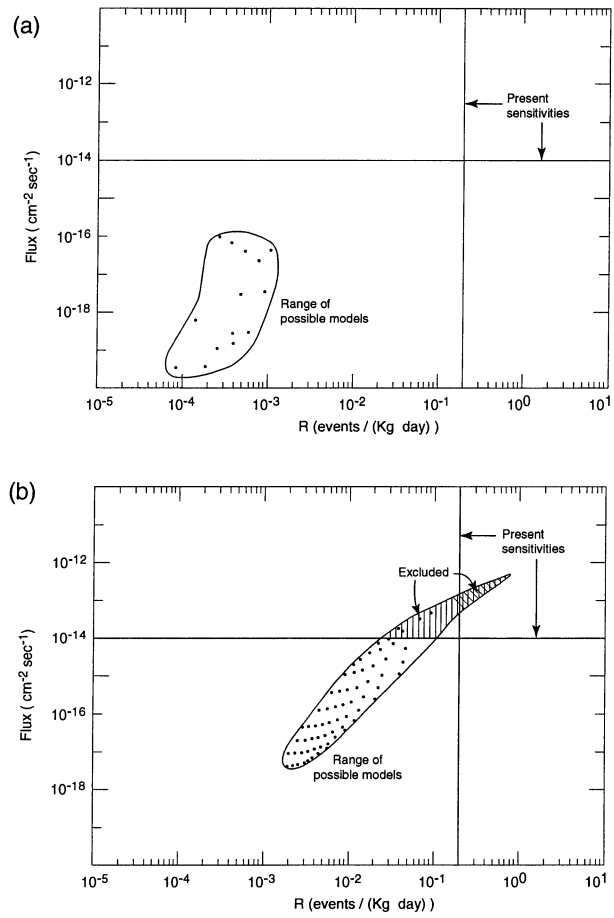


Figure 19: The sensitivities of direct and indirect searches for dark matter in (a) “universal” models, and (b) “non-universal” models ?.

high-energy annihilation neutrinos – may have a realistic chance of uncovering the dark matter of the Universe.

1. J. Ellis, Lectures presented at the Les Houches Summer School on “Cosmology and Large Scale Structure”, Summer 1993, CERN Preprint TH. 7083/93 (1993).
2. See, e.g., C.J. Copi and D.N. Schramm, astro-ph/9504026; M. Bolte and C.J. Hogan, *Nature* **376** (1995) 399.
3. J. Ellis, *Nucl.Phys.* **B48** (1996) 522.
4. W. Fowler and F. Hoyle, *Ap.J.Supp.* **9** (1964) 201; R. Wagoner, *Astrophys.J.* **179** (1973) 343.
5. Relatively high values of (or upper limits on) the Deuterium abundance have recently been reported in Lyman  $\alpha$  clouds at high redshifts: R.F. Carswell et al., *MNFAS* **268** (1994) L1; A. Songaila et al., *Nature* **368** (1994) 599; M. Rugers and C.J. Hogan, astro-ph/9512004. However, there is also a report of a relatively low value of the Deuterium abundance: D. Tytler and X. M. Fan, *Bull. AAAS* **26** (1994) 1424, and the hope that these observations might yield measurements of the primordial Deuterium abundance is cast into doubt by indications that nuclear processing may be important already at these early times: E.J. Wampler et al., astro-ph/9512084.
6. K.A. Olive, astro-ph/9609071, and references therein.
7. E.W. Kolb and M.S. Turner, “The Early Universe” (Addison-Wesley, Redwood City, 1990).
8. J. Ellis and G. Steigman, *Phys.Lett.* **89B** (1980) 186.
9. A.D. Sakharov, *Pis'ma Zh.Eksp.Teor.Fiz.* **5** (1967) 32.
10. J.H. Applegate and C.J. Hogan, *Phys.Rev.* **D31** (1985) 3037; J.H. Applegate, C.J. Hogan and R. Scherrer, *Phys.Rev.* **D35** (1987) 1151; C. Alcock, G.M. Fuller and G.J. Mathews, *Astrophys.J.* **320** (1987) 439.
11. Y. Iwasaki et al., *Phys.Rev.* **D46** (1992) 4657; B. Grossmann and M.L. Laursen, Jülich Preprint HLRZ-93-7 (1993); Y. Iwasaki et al., CERN Preprint TH. 6798/93 (1993).
12. D. Thomas, D.N. Schramm, K.A. Olive and B.D. Fields, *Ap.J.* **406** (1993) 569.
13. A.A. Starobinsky, *Phys.Lett.* **91B** (1980) 99; A. Guth, *Phys.Rev.* **D23** (1981) 349.
14. A. Guth and E. Weinberg, *Phys.Rev.* **D23** (1981) 876;

- S.W. Hawking, I.G. Moss and J.M. Stewart, *Phys.Rev.* **D26** (1982) 2681.
15. A.D. Linde, *Phys.Lett.* **108B** (1982) 389;  
A. Albrecht and P.J. Steinhardt, *Phys.Rev.Lett.* **48** (1982) 1220.
  16. A.D. Linde, *Phys.Lett.* **129B** (1983) 177.
  17. J. Bardeen, P.J. Steinhardt and M.S. Turner, *Phys.Rev.* **D28** (1983) 679;  
A.H. Guth and S.-Y. Pi, *Phys.Rev.Lett.* **49** (1982) 1110;  
A.A. Starobinsky, *Phys.Lett.* **117B** (1982) 175;  
S.W. Hawking, *Phys.Lett.* **115B** (1982) 295.
  18. N.D. Birrell and P. Davies, "Quantum Fields in Curved Space" (Cambridge University Press, Cambridge, 1982).
  19. J.R. Bond, Lectures at the Les Houches Summer School on "Cosmology and Large Scale Structure", Summer 1993.
  20. I.J. Grivell and A.R. Liddle, astro-ph/9607096, and references therein.
  21. G. Smoot et al., *Astrophys.J.* **360** (1990) 685 and **369** (1992) L1;  
C.L. Bennett et al., *Astrophys.J.* **391** (1991) and **436** (1994) 423.
  22. C.L. Bennett et al., COBE Preprint 96-01, astro-ph/9601067.
  23. G. Hinshaw et al., COBE Preprint 96-04, astro-ph/9601058;  
E.L. Wright et al, astro-ph/9601059.
  24. A. Kogut et al., COBE Preprint 96-07, astro-ph/9601062.
  25. M. Tegmark, astro-ph/9601077.
  26. M.S. Turner and N. Vittorio, Talks at the Les Houches Summer School on "Cosmology and Large Scale Structure", Summer 1993.
  27. MACHO Collaboration. C. Alcock et al., *Phys.Rev.Lett.* **74** (1995) 2867;  
EROS Collaboration, E. Aubourg et al., *Astron. Astrophys.* **301** (1995) 1, and R. Ansari et al., astro-ph/9511073.
  28. D. Bennett et al., astro-ph/9510104.
  29. F.C. Adams and G. Laughlin, astro-ph/9602006.
  30. E.I. Gates, G. Gyuk and M.S. Turner, *Astrophys.J.* **449** (1995) L123.
  31. J.P. Ostriker, *Ann.Rev.Astron.Astrophys.* **31** (1993) 689.
  32. R. Brandenberger, "Current Trends in Astrofundamental Physics", eds. N. Sanchez and A. Zichichi (World Scientific, Singapore, 1993), p. 272.
  33. M. White, D. Scott and J. Silk, *Ann.Rev.Astron.Astrophys.* **32** (1994) 319 and *SCIENCE* **268** (1995) 829;  
M. White and D. Scott, astr-ph/9601170.
  34. R.K. Schaefer and Q. Shafi, *Nature* **359** (1992) 119;  
M. Davis, F.J. Summers and D. Schlegel, *Nature* **359** (1992) 393;  
A.N. Taylor and M. Rowan-Robinson, *Nature* **359** (1992) 396.
  35. BW Lee and S. Weinberg, *Phys.Rev.Lett.* **39** (1977) 165;  
P. Hut, *Phys.Lett.* **69B** (1977) 85.
  36. S. Dimopoulos, *Phys.Lett.* **B246** (1990) 347.

37. Particle Data Group, R.M. Barnett et al., *Phys.Rev.* **D54** (1996) 1.
38. T. Yanagida, Proc. Workshop on the Unified Theory and the Baryon Number in the Universe (KEK, Japan, 1979);  
R. Slansky, talk at Sanibel Symposium, Caltech Preprint CALT-68-709 (1979).
39. R. Barbieri, J. Ellis and M.K. Gaillard, *Phys.Lett.* **90B** (1980) 249.
40. B.T. Cleveland et al., *Nucl.Phys.Proc.Supp.* **38** (1995) 47;  
R. Davis *Prog.Part.Nucl.Phys.* **32** (1994) 13, and talk at the Les Houches Summer School on “Cosmology and Large Scale Structure”, Summer 1993;  
Kamiokande Collaboration, Y. Suzuki, *Nucl.Phys.Proc.Supp.* **B38** (1994) 54 and talk by Y. Totsuka at the Les Houches Summer School on “Cosmology and Large Scale Structure”, Summer 1993;  
SAGE Collaboration, J.N. Abdurashitov et al., *Phys.Lett.* **B328** (1994) 234 and talk at V.N. Gavrin at the Les Houches Summer School on “Cosmology and Large Scale Structure”, Summer 1993;  
GALLEX Collaboration, P. Anselmann et al., *Phys.Lett.* **B327** (1994) 377 and **B342** (1995) 440 and talk by R. Bernabei at the Les Houches Summer School on “Cosmology and Large Scale Structure”, Summer 1993.
41. Superkamiokande Collaboration, Y. Totsuka, ICCR Report 227-90-20 (1990) and talk at the Les Houches Summer School on “Cosmology and Large Scale Structure”, Summer 1993.
42. N. Hata and P. Langacker, *Phys.Rev.* **D52** (1995) 420.
43. L. Wolfenstein, *Phys.Rev.* **D17** (1978) 2369;  
S.P. Mikheyev and A.Yu. Smirnov, *Nuovo Cimento* **9C** (1986) 17.
44. See, e.g.: G. Efstathion, J.R. Bond and S.D.M. White, *Mon.Not.R.Ast.Soc.* **258** (1992) 1P; and  
M.S. Turner, FNAL Preprint Conf-92/313-A (1992).
45. Y. Fukuda et al., *Phys.Lett.* **B335** (1994) 237.
46. CHORUS Collaboration, N. Armenise et al., CERN-SPSC/90-42 (1990);  
NOMAD Collaboration, P. Astier et al., CERN-SPSC/91-21 (1991).
47. M. Fukugita and T. Yanagida, *Phys.Lett.* **174B** (1986) 45.
48. V. Kuzmin, V. Rubakov and M. Shaposhnikov, *Phys.Lett.* **155B** (1985) 36.
49. J. Ellis, J. Lopez, D.V. Nanopoulos and K.A. Olive, *Phys.Lett.* **B308** (1993) 70.
50. J. Ellis and P. Sikivie, *Phys.Lett.* **B321** (1994) 390.
51. H. Goldberg, *Phys.Rev.Lett.* **50** (1983) 1419;  
J. Ellis, J.S. Hagelin, D.V. Nanopoulos, K.A. Olive and M. Srednicki,

- Nucl.Phys.* **B238** (1984) 453.
52. H.E. Haber and G.L. Kane, *Physics Reports* **117** (1985) 75.
  53. J. Ellis, T. Falk, K.A. Olive and M. Schmitt, hep-th/9606292.
  54. J. Ellis and R. Roszkowski, *Phys.Lett.* **B283** (1992) 252.
  55. ALEPH Collaboration, D. Buskulic et al., CERN-PPE/96-83 (submitted to *Zeitschrift für Physik*).
  56. S. Kelley et al., *Phys.Rev.* **D47** (1993) 2461.
  57. L. Bergström and P. Gondolo, Uppsala University Preprint UUITP-17/95 (1995).
  58. V. Berezhinskii et al., *Astropart.Phys.* **5** (1996) 1, and CERN Preprint TH. 96-42, hep-ph/9603342.
  59. T. Falk, K.A. Olive and M. Srednicki, *Phys.Lett.* **B354** (1995) 99.
  60. J. Silk and M. Srednicki, *Phys.Rev.Lett.* **53** (1984) 624.
  61. L. Bergstrom, *Nucl.Phys.* **B325** (1989) 647;  
S. Rudaz and F. Stecker, Minnesota Preprint UMN-TH-823/90 (1990).
  62. J. Silk, K.A. Olive and M. Srednicki, *Nucl.Phys.* **B279** (1987) 804.
  63. A. Gould, *Ap.J.* **321** (1987) 571.
  64. EMC Collaboration, J. Ashman et al., *Nucl.Phys.* **B328** (1989) 1.
  65. G. Jungman, M. Kamionkowski and K. Griest, *Physics Reports* **267** (1996) 195.
  66. F. Halzen, astro-ph/9508020.
  67. M. Goodman and E. Witten, *Phys.Rev.* **D30** (1985) 3059.
  68. J. Ellis and R.A. Flores, *Phys.Lett.* **B263** (1991) 259; *Nucl.Phys.* **B400** (1993) 25.
  69. J. Engel and P. Vogel, *Phys.Rev.* **D40** (1989) 3132.
  70. J. Ellis and R.A. Flores, *Nucl.Phys.* **B307** (1988) 883.
  71. A.F. Pacheco and D. Strottmann, *Phys.Rev.* **D40** (1989) 2131;  
F. Iachiello, L. Krauss and G. Maino, *Phys.Lett.* **B254** (1991) 220.
  72. J. Ellis and R.A. Flores, *Phys.Lett.* **B263** (1991) 259.